Oil Film Behavior Near The Onset Of Flow Reversal In Immiscible Gas/Liquid Vertical Annular Flow

P. L. Blankenberger
University of Wisconsin-Madison

A. S. Miller
University of Wisconsin-Madison

T. A. Shedd
University of Wisconsin-Madison

R12-3

OIL FILM BEHAVIOR NEAR THE ONSET OF FLOW REVERSAL IN IMMISCIBLE GAS/LIQUID VERTICAL ANNULAR FLOW

Patricia L. Blankenberger, Graduate Research Assistant, University of Wisconsin-Madison,
1500 Engineering Drive, Madison, WI 53706, USA; Phone: 608/265-2287; Fax: 608/262-8464
E-Mail: blanken@sel.me.wisc.edu *Author for Correspondence

Audrey S. Miller, Undergraduate Research Assistant, University of Wisconsin-Madison,
1500 Engineering Drive, Madison, WI 53706, USA; Phone: 608/265-2930; Fax: 608/262-8464
E-Mail: audreymiller@students.wisc.edu

Timothy A. Shedd, Assistant Professor, University of Wisconsin-Madison,
1500 Engineering Drive, Madison, WI 53706, USA; Phone: 608/265-2930; Fax: 608/262-8464
E-Mail: shedd@engr.wisc.edu

An important design problem in large refrigeration and air-conditioning systems is the sizing of large diameter vertical pipes optimized to allow liquid to be forced up the pipe walls with minimum overall pressure loss. Of particular concern is the ability of refrigerant vapor flow to drive a liquid oil film through a refrigerant circuit so that oil does not accumulate outside the compressor under normal operation. This paper describes a study aimed at characterizing the dynamic behavior of an annular oil film layer driven by air upward through a 50.8 mm pipe. An optical film thickness sensor is used to obtain liquid thickness data for a matrix of air and oil flow rates. The film thickness and gas mass flow at which flow reversal occurs are presented. Flow reversal in the oil film layer is identified both visually and by particle streak tracking to eliminate ambiguity and subjectivity. These results are compared and discussed with previously published experimental data and modeling work.

INTRODUCTION

Oil is needed in refrigeration systems for lubrication and sealing within the compressor. Screw compressors are typically designed to be oil flooded as a principle means for sealing the rotors. As a result, oil carry-over in the discharge line from screw compressors tends to be very, high requiring the use of oil separators for reducing the concentration allowed to migrate out to system heat transfer components. Since oil separators are not 100% effective at removing liquid, some oil will be carried-over to the system.

Oil in reciprocating compressors is distributed by either a splash or force-fed pumping system to provide lubrication of moving parts. Since the carry-over of oil in the discharge line from reciprocating compressors tends to be much lower as compared to screw compressors, most systems with reciprocating compressors are not equipped with external oil separation devices. However, oil can and will escape out into the system. This will happen mainly during start-up of the compressor. The refrigerant in the system undergoes a rapid expansion at start-up, throwing oil and refrigerant to the piston cylinder walls. The pistons cannot return the large amounts of oil thrown to the wall back to the crankcase of the compressor, so a large amount of oil can be pumped through the refrigeration system. The oil that is now mixed in with the refrigerant must be pulled by the refrigerant through the entire refrigeration system and back to the compressor. If the refrigerant cannot impart enough momentum to the oil to return it to the compressor crankcase, the compressor will not have enough lubrication during operation and will likely be damaged. Therefore, determining the appropriate refrigerant vapor flow rate is important for keeping the system running efficiently.

A major design concern of large refrigeration systems or chillers is the sizing of the vertical risers in the system to have a minimal pressure drop for the critical refrigerant flow through these risers (critical flow meaning the flow required to bring the oil in the refrigerant to the top of the riser). These can be large pipes (on the order of 50.8 mm) and substantial refrigerant flow is required in order to raise the oil in the system to the top of the riser to move the oil through the system. Flooding, or flow reversal, happens when the refrigerant flow is not great enough to drag the oil to the top of the riser.

Mehendale and Radermacher (2000) determined the refrigerant mass flow rate at which reversal occurs using sight glasses in the test section. They developed an analytical model to predict the onset of film flow reversal in annular two-phase flow assuming the refrigerant core and the liquid film were linked by the Wallis interfacial friction factor. Flow reversal was assumed to occur when the wall shear stress went to zero in their model. They predicted that as the film thickness increased, the critical refrigerant mass flow rate decreased, and that the critical refrigerant flow rate increased as the pipe diameter increased. This model also predicted that as the oil concentration in the circulating refrigerant increased, the oil film thickness would increase and, therefore, that the critical refrigerant flow rate would decrease.

For a given pipe geometry and fluid physical properties, the flow reversal transition appears to occur at an approximately constant vapor flow rate, independent of the liquid flow rate (Hewitt, 1977). Wallis (1969) and Jacobs, et al. (1976) suggest using the following parameters to determine flow reversal transitions

$$j_g^* = j_g \, \rho_g^{1/2} \, [gD(\rho_f - \rho_g)]^{-1/2} \, , \tag{1}$$

$$j_f^* = j_f \, \rho_f^{1/2} \, [gD(\rho_f - \rho_g)]^{-1/2}, \tag{2}$$

$$j_g^{*1/2} + m \, j_f^{*1/2} = C, \qquad \text{(correlation for flooding)} \tag{3}$$

where j_g and j_f are the superficial velocities, ρ_g and ρ_f are the densities of the gas and liquid, and D is the diameter of the pipe (Wallis, 1969). The empirical constants m and C depend on the liquid viscosity (Jacobs, et al., 1976) and have values of 1.0 and 0.88, respectively (Vijayan, 2001). It was thought that flooding (or flow reversal) would occur at j_g*=1 (Hewitt, 1977) or j_g*=0.85 (Jacobs, et al., 1976). However, it should be noted that, Jacobs, et al. do not recommend using this criterion for pipes having a diameter greater than 5 cm.

Vijayan et al. (2000) discovered that there were several forms of liquid flow behaviors during flooding, including a ring type wave in small pipes and a churning flow behavior in larger pipes. Vijayan et al. used both Hewitt-Wallis' correlation, Eqns. (1-3), and Kutateladze's correlation, Eqns. (4-5), to analyze their data of air-water flow through pipes of several diameters. It was found that Hewitt-Wallis' correlation agreed well with the small diameter pipe data, and that Kutateladze's correlation agreed well with data from the larger diameter pipes. The Kutateladze type correlation is

$$Ku_g^{*\,1/4} + C_1 Ku_f^{*\,1/4} = C_2, \tag{4}$$

where are dimensionless gas and liquid superficial velocities given by

$$Ku_g^* = u_g[\rho_g^{\,2} / (g\sigma(\rho_f - \rho_g))]^{1/4} \quad \text{and} \quad Ku_f^* = u_f[\rho_f^{\,2} / (g\sigma(\rho_f - \rho_g))]^{1/4} \tag{5}$$

and C_1 and C_2 have the values 1.0 and 1.79, respectively (Vijayan et al., 2001).

A review of the previous research found that determining the point at which the vertical flow reverses has mainly been done by visual observation. According to Hewitt (1977), the methods of determining a flow regime visually are mainly subjective and very often require high speed photographic techniques to capture high speed flow patterns. The transition point can be very difficult to identify accurately using only subjective visual techniques.

In this work, a flow of dry air and oil (soybean, density=920 kg/m^3, viscosity=0.04 kg/m-s) was used in a 50.8 mm pipe to study the behavior of immiscible vapor/liquid systems. The film thickness was measured optically over a range of flows and flow visualization was used to determine the flow behavior at various flow combinations of oil and air near the onset of flow reversal.

EXPERIMENTAL SETUP

The experimental apparatus centers on a clear vertical 1.8-meter long test section (50.8 mm diameter), as shown in Figure 1. Dry compressed air enters the test section at the lower end and flows upward. The oil inlet is also at the lower end and allows the oil to mix with the air before entering the test section. The oil is pumped by a peristaltic pump into a perforated length of tubing inside a tee section at the riser base. The oil flow is measured with a volumetric floating-ball flow meter. After exiting the test section, the air/oil mixture flows into a separator after which the air is vented to the lab exhaust and the recovered oil falls by gravity into an oil reservoir. The separator is designed to use gravity, centrifugal effects, and a coalescing filter to separate the oil from the air.

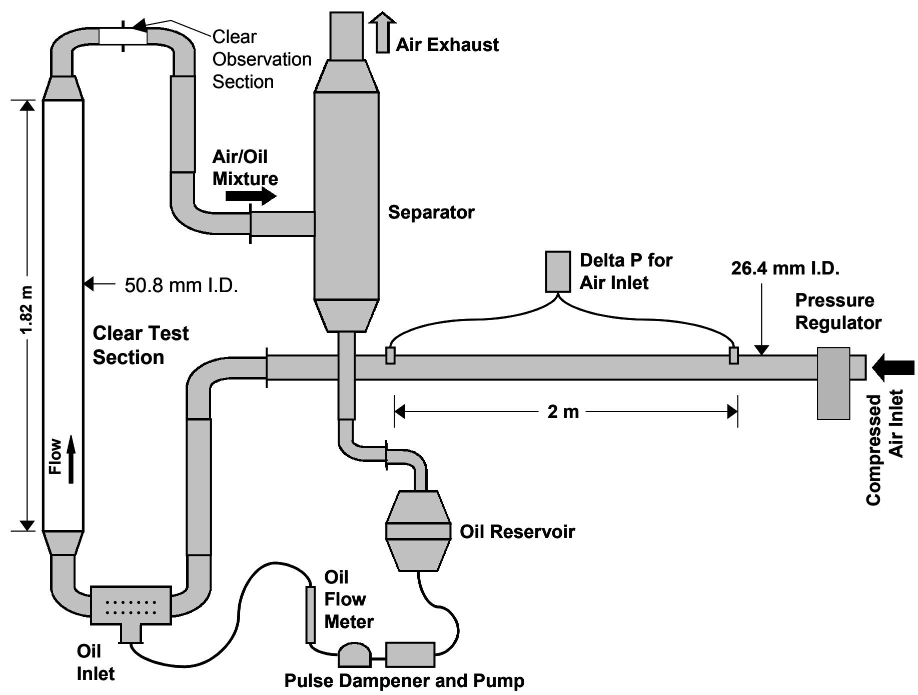

Figure 1: *Experimental Test Set Up*

The volumetric flow rate of the air was determined by measuring the pressure drop across a 2 m length of the entrance pipe. The Colebrook relation for turbulent friction factor (Colebrook, 1938-39),

$$\frac{1}{f^{0.5}} = -2.0\log\left(\frac{e/D}{3.7} + \frac{2.51}{\mathrm{Re}\, f^{0.5}}\right) \tag{6}$$

(where e is the wall roughness and D is the hydraulic diameter), the relation between pressure drop and friction factor,

$$\Delta P = f\left(\frac{\rho V^2}{2}\right)\left(\frac{L}{D}\right) \tag{7}$$

(where ΔP is the pressure drop and L is the distance between pressure taps), together with the definition of the Reynolds, were then solved simultaneously to provide the volume flow rate of air in the loop. This process was simplified and automated by using the EES equation solver software package (F-Chart Software, 2002). The theoretical uncertainties in this method are estimated to be 3.1% (Rush et al., 1999); uncertainty analysis of the current experiment predicted an average uncertainty of ±0.00045 kg/s. Calibration to a NIST-traceable thermal volumetric flow meter (Thermal Systems Incorporated) gave agreement to within 5%.

The oil volumetric flow meter was calibrated by timing how long it took to fill a graduated cylinder with 160 mL of oil. The uncertainty of the flow meter is ±0.02 L/min at a reading of 0.4 L/min or lower and an uncertainty of 5% of the reading above 0.4 L/min.

Film thickness measurements were taken using an optical method (Shedd and Newell, 1995). This method involves shining a small circular light source (such as a light emitting diode, or LED) through the pipe wall and liquid film. The light will be refracted and reflected by the liquid film, creating a ring of light on the pipe wall. The diameter of the light ring is proportional to the thickness of the liquid film. Using geometry and the indices of refraction for the pipe wall and the liquid, the film thickness can be determined. The uncertainty in the film thickness measurement is ±0.034 mm.

Particle streak tracking was also used to investigate the flow patterns. Video clips were taken while flashing a strobe light and a set of three different colored LED lights. The three different colors indicate flow direction, and the strobe light indicates the size of bubbles and waves. Individual frames of the video can be analyzed for flow behavior and to obtain particle velocities.

RESULTS

At each oil flow rate, as the air flow was decreased from a rate that produced a definite up-flow of oil to a definite down-flow of oil, a churning ridge or ring of oil became visible in the test section. This churning ring of oil appeared at flow rates close to the onset of flow reversal and would remain stationary if the air flow was not lowered further. With slight decreases in air flow, the churning oil ring began to recede down the pipe (in the direction of the gravity force). The amount of oil being pushed up through the test section could be viewed in the clear pipe in the return pipe after the test section. It is interesting to note that significant oil flow was observed in the return pipe even after the oil ridge (or definite down flow) appeared in the test section. This oil flow appeared to be due to droplets being entrained in the gas stream and being carried out of the test section.

Film thickness measurements, shown in Figure 2, were taken at several flow conditions while the flow was being lowered from definite up-flow to definite down-flow of oil. More film thickness measurements were taken about the churning oil ridge point. The lowest data point for each oil mass flow rate was taken after the churning oil ridge had passed and basically shows a falling film of oil. Measurement uncertainties are illustrated in Figure 2 to show their relative size; for clarity, they are shown on a single data point only.

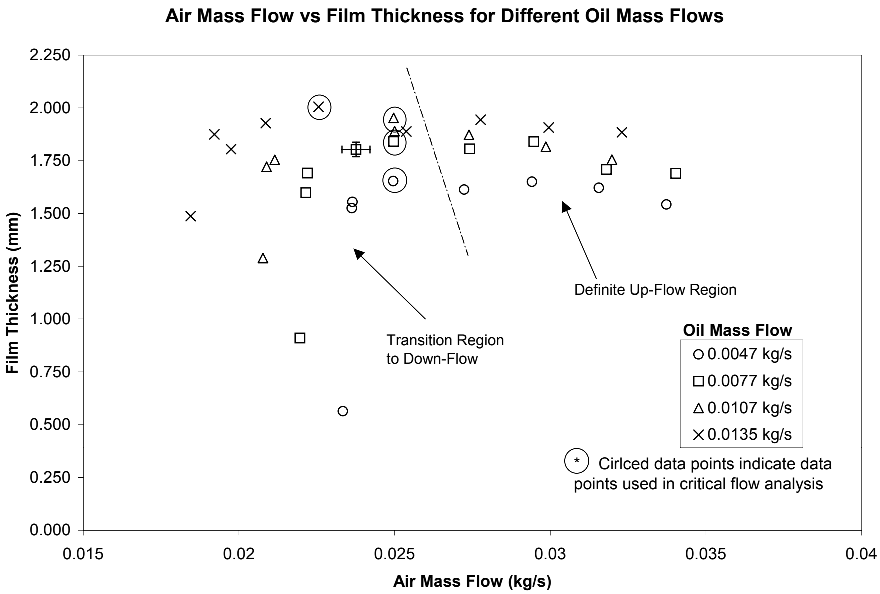

Figure 2: *Film thickness data for various flow conditions of air and oil*

This experiment presented an unexpected flow pattern for the vertical flow. The liquid oil film along the pipe wall appeared to be saturated with small vapor bubbles. We hypothesize that the majority of the bubbles were probably entrained at the oil inlet located at the riser base. Analyzing video images of the flow reveals that the bubbles inhabit a layer of fluid close to the wall. There is another layer of fluid between the inner layer and the core air flow in which a wave flow pattern is exhibited. It seemed that the majority of the bubbles appeared to be only in the inner layer of oil. This is significant because the bubbles could be seen to be moving downward (in opposition to the flow) for nearly all air flow rates. At very high air flow rates, the bubbles (and the inner layer of oil) appeared to be moving very slowly upward, or basically standing still. Waves of oil, like those shown in Figure 3, were drawn upward with the air flow. The waves changed the direction of the bubble movement, causing upward flow for an instant as they passed. In between each wave the bubbles continued to move downward. This can be seen in the particle streak images of Figure 4. The waves appeared to be the primary means of oil mass transport to the top of the pipe in up-flow.

Figure 3: *Waves in Vertical Air/Oil Flow*

Figure 4 shows the use of particle streak tracking to determine the direction of a bubble as a wave passes. A three-color LED strobe light with variable pulse width was used to generate the streak images. The order of flashing of the LEDs was white, red, blue. Figure 4 (a) was taken as a wave passed over, dragging a bubble upward. Figure 4 (b) is the next frame of the video (33 ms later), after the wave has passed. It can be seen here that the flow was downward for all bubbles in the frame. The bubbles shown are slightly out of focus due to the speed of the flow and the flashing of the LEDs. This demonstrates the flow behavior of the film layer closer to the wall (bubble layer), the layer of oil above this (the wave layer), and the interactions between the two.

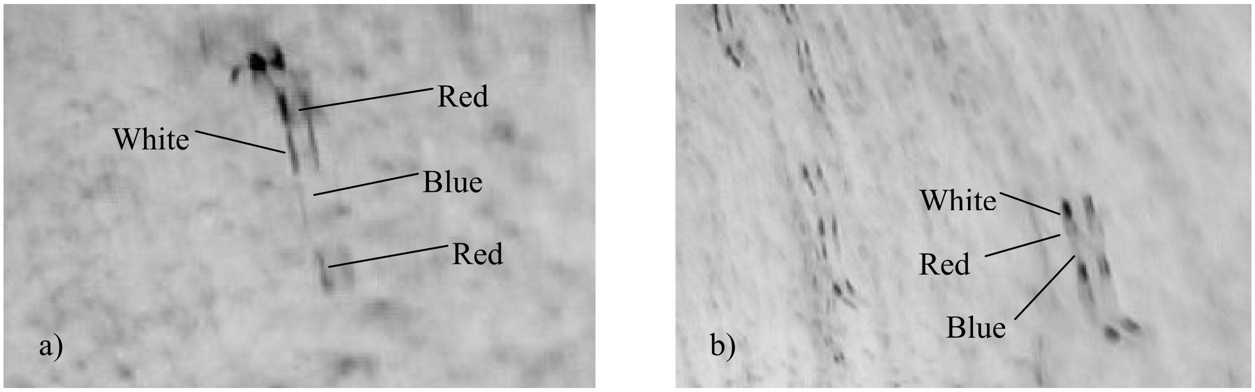

Figure 4: *(a)Bubble caught by a wave and flowing upward (b)Bubble just after a wave passes, moving downward (taken just after (a)) (direction of flow is white, red, blue)*

DISCUSSION

Mehendale and Radermacher (2000) created a model for predicting the film thickness and the vapor velocity required to drive the liquid film up the pipe. In their model they predicted that as the film thickness increased, the amount of vapor required for flooding to occur decreased. The film thickness data found in this experiment, shown in Figure 2, support these findings. In general, for a given air flow rate, as the oil mass flow rate increases, the oil film thickness increases. At low air flows, the film appeared to become so thick that the interface was unstable, leading to a localized churning motion. Above this ring of churning liquid, a smooth, gravity-driven film fell down the pipe. Below it, the waves on the film appeared to be moving upward, while the bubbles in the inner layer maintained a general downward motion. The air flow at which the churning ring moved beyond the top of the test section was considered to be the critical air mass flow rate for upward liquid flow. The observation of the inverse relationship between the film thickness and the critical vapor mass flow rate may be supported by the theory that there is a critical liquid mass flow rate (inversely proportional to gas velocity) that must be reached before waves will form on a liquid film (Schadel and Hanratty, 1989).

An attempt was made to fit the data to the Wallis-Hewitt correlation shown in Eqns. (1-3). It was found that this correlation over-predicted the vapor velocity required for flooding. Hewitt (1977) suggested that flooding would occur at a value of j_g*=1, and Jacobs et al. (1976) suggested that j_g*=0.85 for use with air-water systems. The value found using the Wallis-Hewitt correlation using m=1.0 and C=0.74 was j_g*=0.47 nearly half of what was suggested by Jacobs et al. However, the constants used in this equation are dependent on the liquid viscosity and therefore should change when using air and oil instead of air and water.

Another attempt was made to fit the data to the Kutateladze correlation, Eqns. (4) and (5), with C_1=1.0 and C_2=1.79 (Vijayan et al., 2001). This correlation over-predicted the flooding velocity by about 53%.

The Feind correlation (Vijayan et al., 2001 and 2002) for determining the film thickness was used to try to predict the flooding film thickness. According to the data found, this correlation under-predicted the film thickness at flooding conditions by a factor of 2.34, or 57%.

An attempt was made to correlate the data using the vapor Reynolds number and the liquid film Reynolds number,

$$Re_g = j_g D/\nu_g \quad \text{and} \quad Re_{LF} = 4m_L/(\pi D \mu_L), \tag{8}$$

respectively, where j_g is the apparent velocity of the vapor, D is the diameter of the test section, ν_g is the kinematic viscosity of the vapor, m_L is the liquid mass flow rate, and μ_L is the liquid viscosity. The correlation found was

$$Re_g = -1033.4\ Re_{LF} + 37394 \tag{9}$$

and is shown in Figure 5. The data point at a Re_{LF}=6.75 was not considered in this curve fit because the pressure reading seemed slightly questionable.

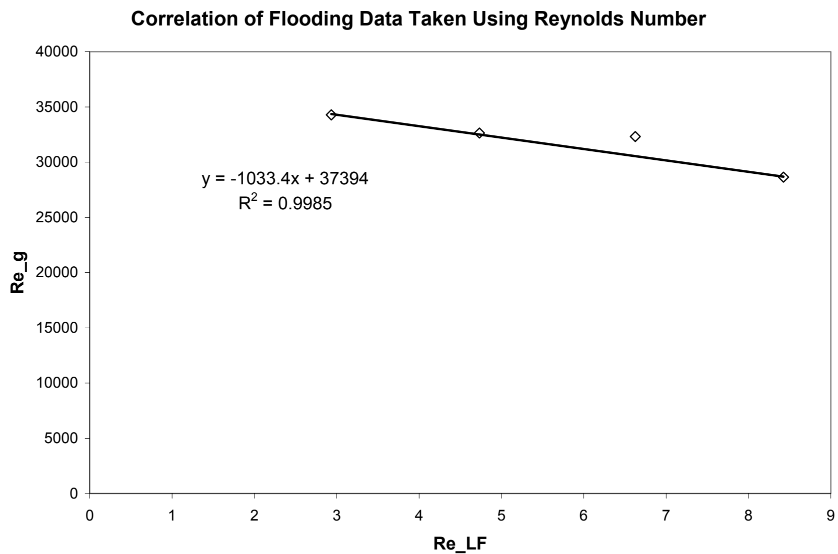

Figure 5: *Possible correlation for flooding data using Reynolds numbers*

While this correlation fit the current data better than those generated from air-water data, it is not necessarily recommended that it be generalized beyond the current experimental conditions. There are other film thickness correlations available, however these require pressure drop data that are not available at this time. These correlations will be tested in future work.

The observation that there seem to be two layers in the liquid film, a bubbly layer along the wall and a wavy layer, was not seen in the literature. The inner, bubbly layer appears to have a downward flow for all air-oil flow combinations studied. The waves appear to be the main mode of mass transfer for the liquid film, after flooding has occurred. (There is significant droplet flow at air velocities below the critical air velocity, and thus some oil still travels to the top of the pipe.)

CONCLUSION

- This experiment supports the model found by Mehendale and Radermacher (2000), which predicts a decrease in the required vapor flow rate for flooding to occur as the liquid flow increases.
- The accepted correlations created using air-water systems do not predict the flow behavior of the air-oil system well. A preliminary correlation was created using Reynolds numbers.
- After observing the flow, there appear to be two separate layers in the liquid film – a bubbly layer along the wall and a wavy layer above this. The waves are thought to be the method of mass transport for the oil upward, whereas bubbles in the inner layer appear to move downward or remain stationary for the most part.

ACKNOWLEDGEMENTS

The authors appreciate the financial support for this project provided by the University of Wisconsin and the National Science Foundation under award number CTS-0134510.

REFERENCES

Colebrook, C. F, "Turbulent Flow in pipes, with particular reference to the transition region between the smooth and the rough pipe laws." *Journal of the Institution of Civil Engineers*, London **11**: 133-156, 1938-39.

F-Chart Software: Engineering Equation Solver (EES). www.fchart.com, 2002.

Hewitt, G. F, "Two-phase flow patterns and their relationship to two-phase heat transfer." In S. Kakac and F. Mayinger, editors, *Two-phase Flows and Heat Transfer*, **volume 1** of *NATO Advanced Study Institute on Two-Phase Flows and Heat Transfer*, pages 11-35. Hemisphere Publishing Company, Washington, D.C., 1977.

Jacobs, M. L.; F. C. Scheideman, S. M. Kazem, and N. A. Macken, "Oil transport by refrigerant Vapor." *ASHRAE Transactions*, **82**(2): 318-329, 1976.

Mehendale, S. S. and R. Radermacher, "Experimental and theoretical investigation of annular film flow reversal in a vertical pipe: application to oil return in refrigeration systems." *HVAC&R Research*, **6**(1): 55-74, 2000.

Rush, T. A., T. A. Newell, and A. M. Jacobi, "An experimental study of flow and heat transfer in sinusoidal wavy passages." *International Journal of Heat and Mass Transfer,* **42**: 1541 – 1553, 1999.

Schadel, S.A. and T.J. Hanratty, "Interpretation of atomization rates of the liquid film in gas-liquid annular flow." *International Journal of Multiphase Flow*, **15**(6): 893-900, 1989.

Shedd, T.A. and T.A. Newell, "Automated optical liquid film thickness measurement method." *Review of Scientific Instruments*, **69**(12): 4205-4213, 1998.

Vijayan, M., S. Jayanti, A.R. Balakrishnan, "Effect of pipe diameter on flooding." *International Journal of Multiphase Flow*, **27**: 797-816, 2001.

Vijayan, M., S. Jayanti, A.R. Balakrishnan, "Experimental study of air-water countercurrent annular flow under post-flooding conditions." *International Journal of Multiphase Flow*, **28**: 51-67, 2002.

Wallis, G.B, *One-Dimensional Two-phase Flow*. McGraw-Hill, New York, 1969.